JOURNAL OF CATALYSIS 85, 349–361 (1984)

Iron Alloy Fischer–Tropsch Catalysts

IV. Reaction and Selectivity Studies of the FeCo System

K. B. ARCURI,[1] L. H. SCHWARTZ,[2] R. D. PIOTROWSKI,[3] AND J. B. BUTT[3]

Ipatieff Laboratory, Northwestern University, Evanston, Illinois 60201

Received February 28, 1983; revised August 1, 1983

Iron–cobalt alloys have been reported to have enhanced C_2–C_3 selectivity in the synthesis reaction for both supported and unsupported materials. Much of the available data are, however, at total pressures of 1 atm and low conversions. This study presents results obtained with a representative $FeCo/SiO_2$ catalyst in comparison with the supported pure metal components at 523°K and pressures up to 14 atm. Major results are that the conversion dependence of selectivity noted at 1 atm is suppressed at higher pressures and the iron-containing materials become good methanol producers at higher pressures, largely at the expense of methane formation. In terms of CO conversion the alloy catalyst resembles Fe/SiO_2 at atmospheric pressure and Co/SiO_2 at higher pressure; however, for oxygenate production just the opposite pertains. The enhanced olefin selectivity for $FeCo/SiO_2$, observed previously in experiments at atmospheric pressure, is not maintained at higher pressures.

INTRODUCTION

A major obstacle in the commercial development of the Fischer–Tropsch synthesis has been control of product selectivity. The hydrocarbon products follow a Storch–Anderson (*1*) weight distribution, thus downstream processing must cope with everything from LPG to heavy wax. Fischer–Tropsch catalysts must be selective toward desirable products (i.e., gasoline, diesel fuel range, or α-olefins) in order for the synthesis to have any commercial viability. Supported alloy catalysts may provide one means of attaining enhanced selectivities compared to classic single component bulk catalysts. Electronic and crystal structure effects can suppress undesirable reactions and alter the relative rates of parallel reactions. For example, Vannice and Garten (*2*) demonstrated that the presence of Pt in a supported FePt bimetallic catalyst altered the synthesis rate of the Fe sites because of electron withdrawal from the iron, while Nakamura *et al.* (*3*) found that an FeCo alloy catalyst produced higher C_2 selectivities than either pure component catalyst.

Overall the Fischer–Tropsch synthesis is a collection of parallel and series reactions that can be broken into primary and secondary categories. We consider CO hydrogenation, α-olefin, and alcohol synthesis to constitute the primary reactions, while water–gas shift, hydrogenation, isomerization, and olefin incorporation are among the secondary reactions. Overall reaction selectivities are influenced by the relative rates of these component reactions and evaluation of catalytic performance requires investigating the relative rates of both primary and secondary reactions. Since the kinetics of each component reaction have different pressure, temperature, and composition dependencies, selectivity comparisons should be made over a range of process conditions in order to evaluate catalyst performance more precisely. The present study focuses on the conversion and pressure dependence of CO activities

[1] Present address: Exxon Research and Development Laboratories, Baton Rouge, Louisiana 70821.

[2] Department of Materials Science and Engineering.

[3] Department of Chemical Engineering.

0021-9517/84 $3.00

TABLE 1

Metal Loading, H_2 Uptake, and Percentage Exposed Metal of the Catalysts

Catalysts	Metal loading (wt%)	H_2 uptake[a] (mol/g)	Metal exposed[b] D_h (%)
Fe	4.94	17.8 ± 0.9	4.7 ± 0.2
Co	4.61	23.1 ± 0.5	6.8 ± 0.2
FeCo	3.85(Fe)[c] 1.02(Co)	22.7 ± 0.9	5.6 ± 0.3

[a] From Amelse *et al.* (*5*).

[b] Based on weight fraction oxide reduced as determined thermogravimetrically. H/metal stoichiometry is 1/1.

[c] Corresponds to an atomic ratio of 80/20: Fe/Co.

and product selectivities of supported Fe, Co, and FeCo catalysts at low CO conversions.

EXPERIMENTAL

Catalyst preparation and characterization. All the catalysts were prepared by nitrate salt impregnation of 80–100 mesh Davison 62 silica gel to incipient wetness. The alloy catalyst was prepared via coimpregnation. After drying at 125°C overnight the samples were calcined in air at 200°C for 2 h and then at 450° for 4 h. Details of the catalyst preparation may be found in Ref. (*4*). Table 1 lists the metal loadings of the catalyst used in this study.

Mössbauer studies conducted in a controlled atmosphere cell revealed that the calcined Fe/SiO_2 was completely reduced in H_2 (425°C, 24 h) to BCC metal and under synthesis conditions (250°C, 1 atm) the reduced catalyst was converted to a mixture of ε' and χ carbide phases (*6*). For the $FeCo/SiO_2$, alloy formation has been verified both via X-ray diffraction and Mössbauer spectroscopy (*7, 8*), although the broad linewidths obtained by both these methods indicate the BCC alloy composition is not uniform. The alloy does not form a carbide phase under synthesis conditions since Co tends to destabilize the bulk iron carbide phase. X-Ray diffraction studies indicated that the calcined oxide of Co/SiO_2 was Co_3O_4 and the reduced catalyst was a mixture of FCC and HCP metallic phases. This catalyst does not form a carbide phase under synthesis conditions. Hydrogen chemisorption was used to determine percentage of metal exposed. The method involves static chemisorption as the temperature is decreased from 450°C to room temperature, flushing in an inert gas (Ar) for 15 min, and then measurement of the amount desorbed upon temperature programming back to 450°C. The method is described in detail by Amelse *et al.* (*5*). This allowed for comparison of activities in terms of CO turnover frequencies. The H_2 uptake values and metal dispersions for each catalyst are given in Table 1. We do not claim that the percentage exposed is a quantitative measure of active sites, but at the least it provides a common basis for comparison.

Reactor system. Rate data were obtained using a ¼-in.-o.d. stainless-steel tube reactor. The interior surface of the reactor was gold plated in order to minimize any wall reactions and/or carbonyl formation. Reactant gases were obtained from Airco Industrial Gases as mixtures of 25% CO (99.3% min purity) in 75% H_2 (99.999% min purity) and 46% CO (99.5% min purity) in 54% H_2 (99.999% min purity). Aluminum feed cylinders were used in order to reduce carbonyl formation. However, low carbonyl concentrations were still observed so a Linde 5-Å sieve trap in a dry ice/acetone bath was also employed in the feed train. Successful carbonyl removal was indicated by the lack of an iron "mirror" on a glass reactor. Feed gas oxygen removal was accomplished by a MnO_2/SiO_2 trap prereduced in flowing H_2. This trap reportedly removes oxygen to less than 1 ppb (*9*).

The reactor pressures employed in this study ranged from 1 to 14 atm at a fixed temperature of 250°C. At the onset of an experiment, the catalyst was reduced for 24 h in flowing H_2 at 425°C. Following reduction the temperature was lowered to 250°C

and the CO/H_2 feed was introduced. The pressure was then quickly brought up to the desired value (normally 1 to 2 min). Kinetic measurements were not taken until the system reached steady state as determined by invariant product compositions as discussed below.

Activity and selectivity were determined via reactant–product analysis using two gas chromatographs in tandem, one for low molecular weight products (C_1–C_4, CO_2, CH_3OH), and the second for higher molecular weight products (normally C_4–C_8). The first employed a Poropak Q column (10 feet × ⅛ in. Supelco, Inc.) and the second a SP 1200 column (10% on Chromosorb, 10 feet × ⅛ in. Hewlett–Packard). Both GC systems employed temperature programming in order to separate the α-olefin/n-paraffin components of each hydrocarbon in approximately 30 min.

In that which follows product yield will be defined as moles of CO converted to product i per mole of feed gas, and selectivity will generally be defined in terms of ratios of turnover frequencies. Run conditions will be designated by catalyst, pressure and feed composition, i.e., Co, 1, 1/1 refers to a run with Co/SiO_2 at 1 atm with 1/1 CO/H_2. It should be noted that the experimental matrix of three catalyst compositions, three pressures, two feed compositions, and a large number of products presents some considerable difficulties for an orderly presentation of results. In the following these are ordered as to overall activity (CO reaction), methane production, olefin production, shift activity, and alcohol production. In all cases the results chosen for illustration are typical of the general trends observed unless identified specifically otherwise.

The experimental procedure involved determining the CO activity and product selectivities as a function of CO conversion level. This was accomplished by varying the gas hourly space velocity (GHSV). Before presenting detailed results, however, it is important to recognize the existence in

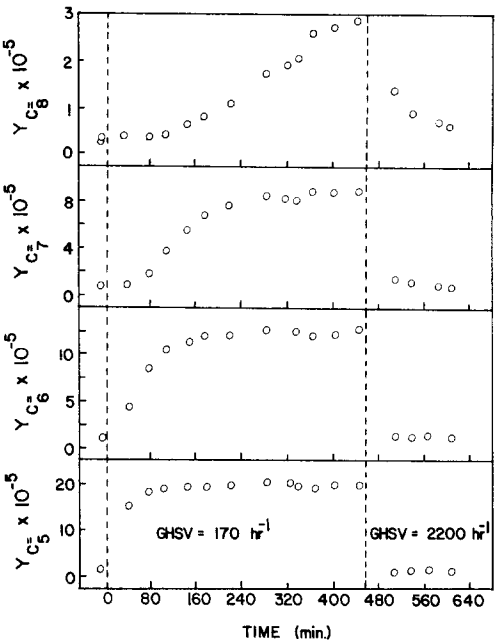

FIG. 1. α-Olefin yields (Y_i) for the C_5 through C_8 products as a function of time during transient experiment for the Fe catalyst at 7.8 atm and 250°C using the 1/1 CO/H_2 feed. At time zero the GHSV was changed from 2200 to 170 h^{-1}.

synthesis studies at higher pressures of long term transients in the product distribution. The effect is particularly pronounced for lower CO/H_2 feed ratios. Some typical results are shown in Fig. 1 for the yields of higher molecular weight products in an experiment with Fe, 7.8, 1/1. At time zero the GHSV was changed from 2200 to 170 h^{-1} and the product composition measured as a function of time. It is seen that the C_5 olefin yield requires about 1.5 h to come to steady state, while the corresponding figure for C_8^{2-} is more than 8 h. There is hysteresis in this effect, since steady conditions were attained much more rapidly when the GHSV was returned to its original high value; this is attributed to the sweeping effect of the higher gas flow. Precise measurements of higher molecular weight distributions thus require considerable experimental patience. Such transients do not have a large effect on values determined for methane turnover frequency (C_1 response is rapid,

TABLE 2

Specific CO Turnover Frequencies (N_{CO}) at Various Pressures and Feed Compositions at 250°C

Pressure (atm)	$N_{CO} \times 10^{-3}$ molecules (site-s[a]) Fe		FeCo		Co	
	1/3	1/1	1/3	1/1	1/3	1/1
1	9.0	3.2	1.7	2.2	45	17
7.8	70.2	21.8	13.3	10.0	13.8	9
14	46.2	47.6	23.8	10.6	24.8	—

[a] At nominal 2% conversion.

less than 0.5 h in the experiment shown) or CO turnover frequency (since the total carbon in higher molecular weight products is relatively small); however, they can lead to significant errors in determination of the distribution parameter. Strictly steady-state conditions pertain to all data presented in this paper.

RESULTS

CO Activities Studies

The CO turnover frequency, N_{CO}, is defined as the molar rate in s^{-1} of CO converted to products (excluding CO_2) per H atom chemisorbed. Presumably the hydrogen chemisorption is a measure of surface Fe. We do not claim that a single surface Fe is the active site, only that the chemisorption measurement provides a common basis for comparison that is preferable to measures such as weight percentage loading.

Table 2 presents the steady-state N_{CO} values obtained for three catalysts as a function of feed composition and pressure. At 1 atm Co is by far the most active, but its N_{CO} decreases with pressure while those of the iron-containing catalysts increase. The relative increase in N_{CO} from 1 to 7.8 atm is greater for 1/3 than for 1/1 feeds, suggesting that the rate is more dependent upon H_2 partial pressure than CO partial pressure, in agreement with previously proposed kinetic models (*10*). At present we have no quantitative explanation for the apparent maximum in N_{CO} for Fe, 7.8, 1/3.

The N_{CO} values, when normalized with respect to total pressure, decrease with increasing pressure as shown in Fig. 2. These are typical results, obtained for FeCo, 1/3. This indicates a combination of nonfirst-order kinetics with respect to hydrogen and strong product inhibition. Previous investigators (*11–13*) have suggested the following kinetic correlation for bulk Fe catalysts at high conversions and pressures greater than 1 atm:

$$N_{CO}/P_{H_2} = kP_{CO}/(P_{CO} + bP_{H_2}) \quad (1)$$

In the present study there was some evidence of deviation from the linear kinetics with respect to P_{H_2} suggested by Eq. (1); however since only two feed compositions were employed the order dependency of the reactants could not be determined quantitatively.

Figure 2 also illustrates the conversion dependence of N_{CO}, reported previously by Amelse *et al.* (*5*). In the present work this functionality was observed for all catalysts and conditions with the exception of Co, 1, 1/3, where N_{CO} was essentially conversion independent. Note, however, that the conversion dependence of N_{CO} is substantially diminished at higher pressures.

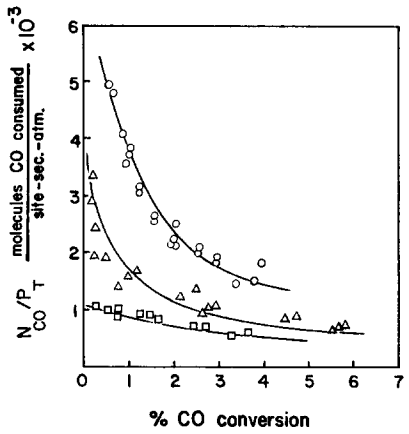

FIG. 2. N_{CO}/P_T versus % CO conversion for the FeCo catalyst as a function of pressure with the 1/1 CO/H_2 feed. ○, △, □ = 1, 7.8, and 14 atm, respectively.

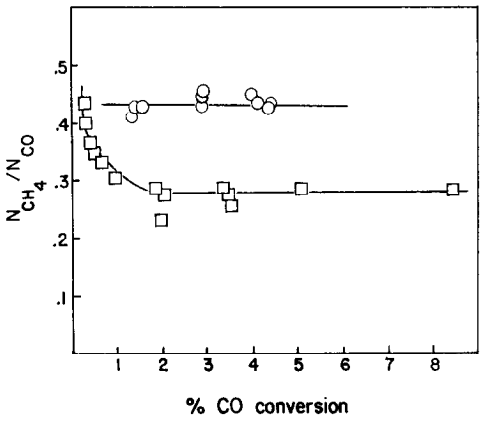

FIG. 3. N_{CH_4}/N_{CO} versus % CO conversion for the Co catalyst at 1 and 14 atm using the 1/3 CO/H_2 feed. ○ = 1, □ = 14 atm.

Activity Maintenance

The observed decrease in CO activity at higher conversion is reversible and not associated with any net loss in catalytic activity. Indeed, in the present work the activity was found constant for periods as long as ca. 40 h. Other workers (*14–18*) have reported significant deactivation, in some cases attributed to the formation of inactive carbonaceous overlayers (*15, 16, 18*). We have observed that iron carbonyl can also deactivate the catalyst, probably also via decomposition to form some type of carbonaceous deposit; it would appear that feed purification via oxygen removal and carbonyl removal as carried out here is sufficient to eliminate rapid initial deactivation.

Methane Selectivity

The methane selectivities, N_{CH_4}/N_{CO} are presented in Fig. 3 for Co, 1, 1/3 and Co, 14, 1/3 and in Fig. 4 for Fe, 1, 1/3; Fe, 14, 1/3; FeCo, 1, 1/3; and FeCo, 14, 1/3. At 1 atm this selectivity decreases with increasing conversion for both iron-containing catalysts but remains constant for the Co catalyst. These results are representative of a general trend noted throughout the work that iron-containing catalysts are more susceptible to product inhibition than Co.

At 1 atm the alloy catalyst yields methane selectivities comparable to Fe, but at higher pressures the selectivity becomes comparable to that of Co and is significantly higher than that of Fe, as shown in Fig. 4. This result, combined with the fact that N_{CO} for FeCo and Co are similar at higher pressures (c.f. Table 2), suggests that the rate of CO consumption and CH_4 production over the alloy catalyst is strongly influenced by Co at higher pressures. Similar results were obtained with the 1/1 feed, however the N_{CH_4}/N_{CO} values were lower due to the higher CO concentrations.

Low Molecular Weight Product Yields and Selectivities

Figure 5 presents ethylene yields for Fe, 1, 1/3, FeCo, 1, 1/3 and Co, 1, 1/3. The FeCo has the best yield behavior and Co the poorest, a result also reported by Naka-

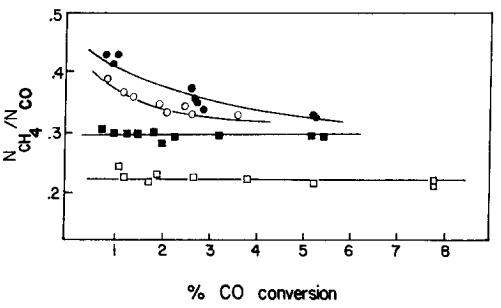

FIG. 4. N_{CH_4}/N_{CO} versus % CO conversion for the Fe and FeCo catalysts using the 1/3 CO/H_2 feed at 1 and 14 atm. T = 250°C, ○, □ = Fe at 1, 14 atm; ●, ■ = FeCo at 1, 14 atm.

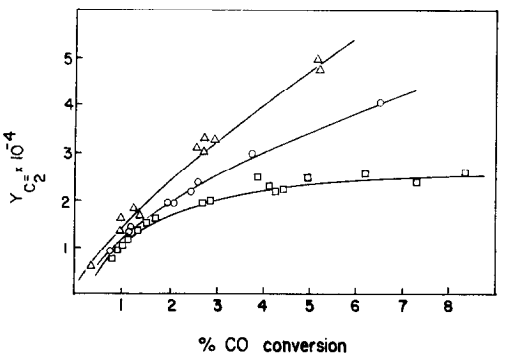

FIG. 5. Ethylene yield versus % CO conversion for the Fe, Co, and FeCo catalysts in the 1/3 CO/H_2 feed at 1 atm and 250°C. □ = Co, ○ = Fe, △ = FeCo.

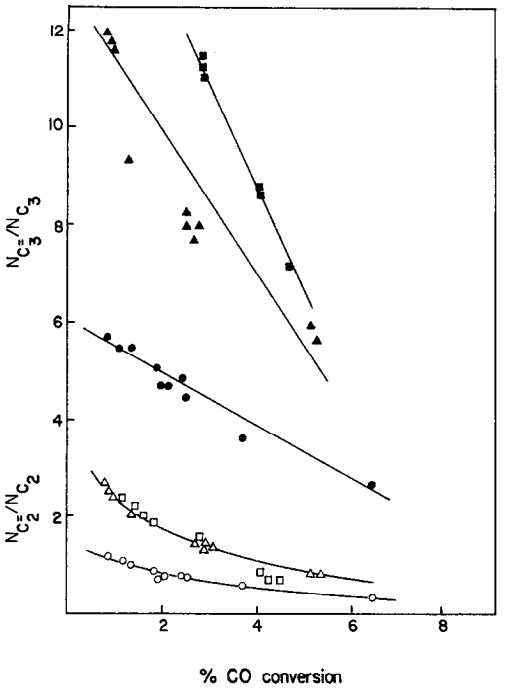

FIG. 6. Propylene/propane and ethylene/ethane ratios versus % CO conversion for all three catalysts at 1 atm with 1/3 CO/H_2 feed. Co = □, ■; FeCo = △, ▲; Fe = ○, ●. Empty symbols refer to C_2 ratios.

mura *et al.* (*3*). However, the ethylene to ethane selectivity, $N_{C_2}{}^{2-}/N_{C_2}$, (Fig. 6) for FeCo, 1, 1/3 is comparable to that for Co, 1, 1/3, while Fe, 1, 1/3 is the lowest. Results on propylene under these conditions are similar, as shown in Fig. 6.

The general influence of pressure on olefin yield and selectivity is shown in Figs. 7 and 8. Yield behavior is typically that shown in Fig. 7 for all three catalysts at 7.8 atm, 1/3 feed. For $Y_{C_2}{}^{2-}$ the relative values are FeCo ~ Fe > Co while for $Y_{C_3}{}^{2-}$, FeCo > Fe ~ Co. There is no significant trend with feed composition. Selectivities, in terms of the ratio of olefin/paraffin turnover numbers, decrease for all three catalysts as pressure is increased. The results at 14 atm, 1/3 feed are illustrated in Fig. 8. Increased hydrogenation efficiency, reflected through increased hydrogen partial pressure, is evidenced by all three catalysts. However, the selectivities at 14 atm for the FeCo are lower than either of the pure component

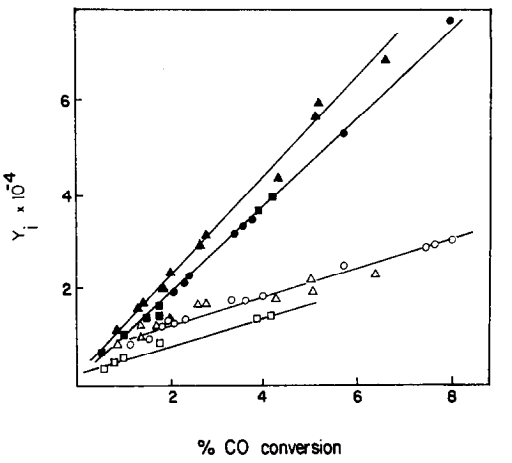

FIG. 7. Ethylene ($Y_{C_2}{}^{2-}$) and propylene ($Y_{C_3}{}^{2-}$) yields versus % CO conversion for all three catalysts at 7.8 atm. ○, ● = Fe; △, ▲ = FeCo; □, ■ = Co. Empty symbols refer to C_{2-}.

catalysts and the prospect of high olefin selectivity for the alloy promised by low pressure results disappears at higher pressures (compare Figs. 6 and 8).

A corollary to these results on olefin yield and selectivity is illustrated in Fig. 9 for $Y_{C_2}{}^{2-}$ as a function of pressure and conversion; results pertain to the Co catalyst

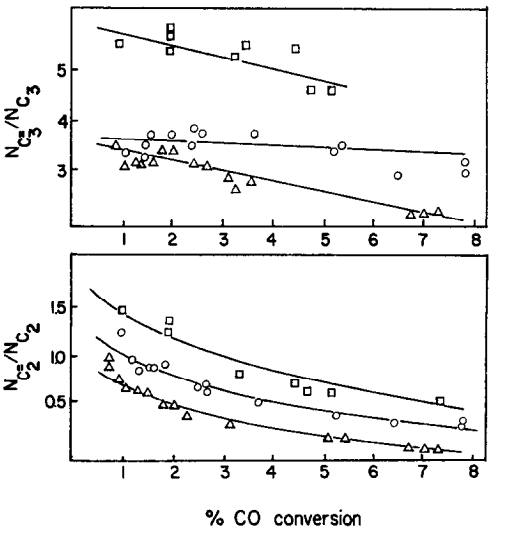

FIG. 8. $N_{C_2}{}^{2-}/N_{C_2}$ and $N_{C_3}{}^{2-}/N_{C_3}$ selectivities versus CO conversion for the Fe, Co, and FeCo catalyst at 14 atm in the 1/3 CO/H_2 mixture. ○ = Fe, △ = FeCo, □ = Co.

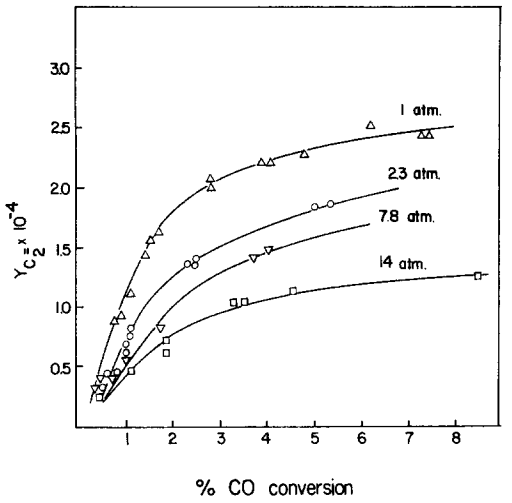

FIG. 9. Ethylene yield versus % CO conversion for the Co catalyst at several pressures using the 1/3 CO/H_2 feed.

but are typical. One can see that an asymptotic value of $Y_{C_2}^{2-}$ is approached at relatively low conversions, the magnitude of which decreases with pressure. The hydrogenation of ethylene cannot solely be responsible for this since, as will be seen later, the product distribution shifts to higher molecular weight molecules with increasing pressure and total C_2 yield decreases. This is consistent with a synthesis mechanism involving ethylene or its surface precursors as active agents in the chain growth reactions and will be treated in detail in a subsequent paper.

Oxygen-Containing Products

The water–gas shift reaction was monitored for all conditions employed in this study. Under low conversion conditions the exit mole fraction ratio CO_2/H_2O can be used to characterize the extent of shift activity. Amelse *et al.* (*5*) previously observed that the FeCo catalyst had a higher shift activity than either pure component catalyst at 1 atm with the 1/3 CO/H_2 feed. Figure 10 presents N_{CO_2}/N_{H_2O} as a function of conversion for the three catalysts at 1 atm with both the 1/1 and 1/3 feeds. The alloy catalyst possesses the highest activity with the 1/3 feed; however, both iron-containing catalysts have comparable activity with the 1/1 CO/H_2 feed at 1 atm. Note that the shift activity of the Co catalyst is independent of the feed composition.

At higher pressures the shift activity of the Fe catalyst is greater than that of the alloy catalyst with the 1/1 feed while both catalysts possess comparable activities with the 1/3 feed (Fig. 11). The Co catalyst (not shown) has the lowest activity with N_{CO_2}/N_{H_2O} values of ca. 0.02–0.03, insensitive to conversion.

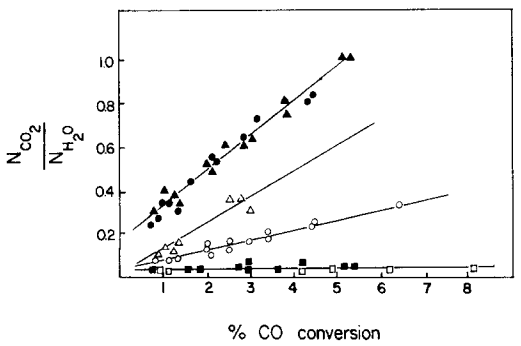

FIG. 10. Shift activity versus % CO conversion for all three catalysts at 1 atm and 250°C using the 1/3 and 1/1 CO/H_2 feeds. ○, ● = Fe; △, ▲ = FeCo; □, ■ = Co. Empty symbols refer to 1/3 feed.

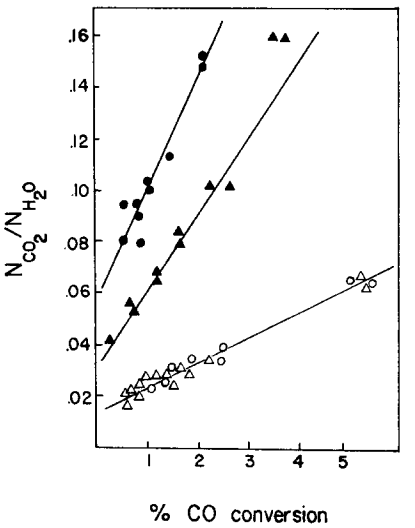

FIG. 11. Shift activity versus % CO conversion for the Fe and FeCo catalysts at 14 atm with the 1/1 and 1/3 CO/H_2 feeds. ○, ● = Fe; △, ▲ = FeCo. Empty symbols refer to 1/3 feed.

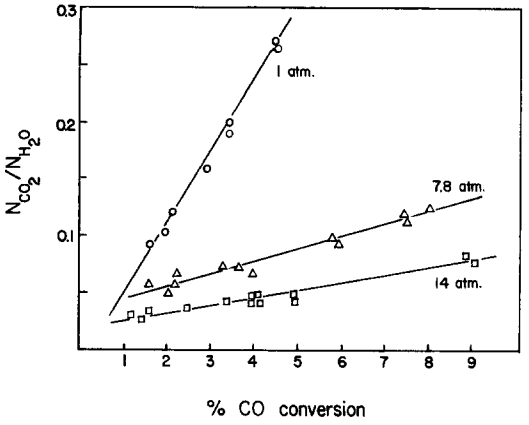

FIG. 12. Shift activity versus % CO conversion for the Fe catalyst at various pressures using the 1/3 CO/H_2 feed at 250°C.

The water–gas shift reaction is not equilibrium limited since for all conditions studied the activity was found to increase with CO conversion. This has been verified via calculation using equilibrium data (*19*) and is also supported by the results of Dry *et al.* (*20*). Typically the N_{CO_2}/N_{H_2O} ratios obtained are approximately 1% of the equilibrium ratios.

Increasing pressure results in a decrease of shift activity, as illustrated in Fig. 12. High pressure integral reactor studies (*11*) and low conversion atmospheric studies (*5, 16*) indicate that water is a primary product in the synthesis. Amelse *et al.* (*5*) demonstrated that the value of N_{CO_2}/N_{H_2O} approaches zero for near zero conversion at 1 atm. Similar trends at higher pressure are indicated by the data of Figs. 11 and 12. This is at least indirect evidence that CO_2 formation via the Boudouard reaction is very slow and is not important in these studies, even though for the feed compositions employed here at 250°C the equilibrium constant is ca. 10^8 at 1 atm (*21*).

Methanol Yields

At higher pressures methanol becomes a dominant synthesis product, second only to methane for Fe and FeCo. The methanol product mole fraction is shown in Fig. 13 at 7.8 and 14 atm. There is a slight decrease in production with yield, but much less than for the CO turnover frequency. Product fractions are ranked Fe > FeCo > Co for 1/3 (Fig. 13); however, FeCo > Fe for 1/1, with Co essentially inactive (Fig. 14). This would indicate that the kinetic dependence of methanol production on CO and H_2 is different for the alloy catalyst than for the pure component materials.

Total Product Distributions

In Figs. 15 and 16 the product mole fractions for FeCo, 14, 1/1 are compared with those for Fe, 14, 1/1 and Co, 14, 1/1. Methanol is the most dominant product after methane for Fe and FeCo, and is produced in largest amount for this feed composition by FeCo. Alcohol yield is about 30% greater for 1/3 feed than for 1/1 feed and the largest amount obtained in any of the ex-

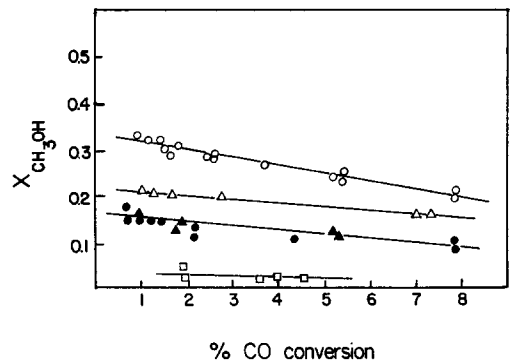

FIG. 13. Methanol product mole fraction versus percent CO conversion for all three catalysts using the 1/3 CO/H_2 feed at 250°C. ●, ○ = Fe at 7.8, 14 atm; ▲, △ = FeCo at 7.8, 14 atm; □ = Co at 14 atm.

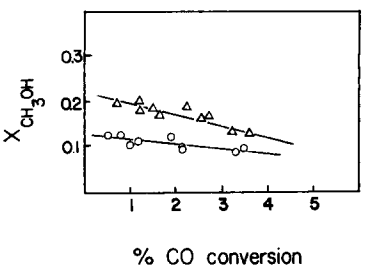

FIG. 14. Methanol product mole fraction versus percentage CO conversion for the Fe and FeCo catalysts using the 1/1 CO/H_2 feed at 250°C. ○ = Fe, 1 atm; △ = FeCo, 14 atm.

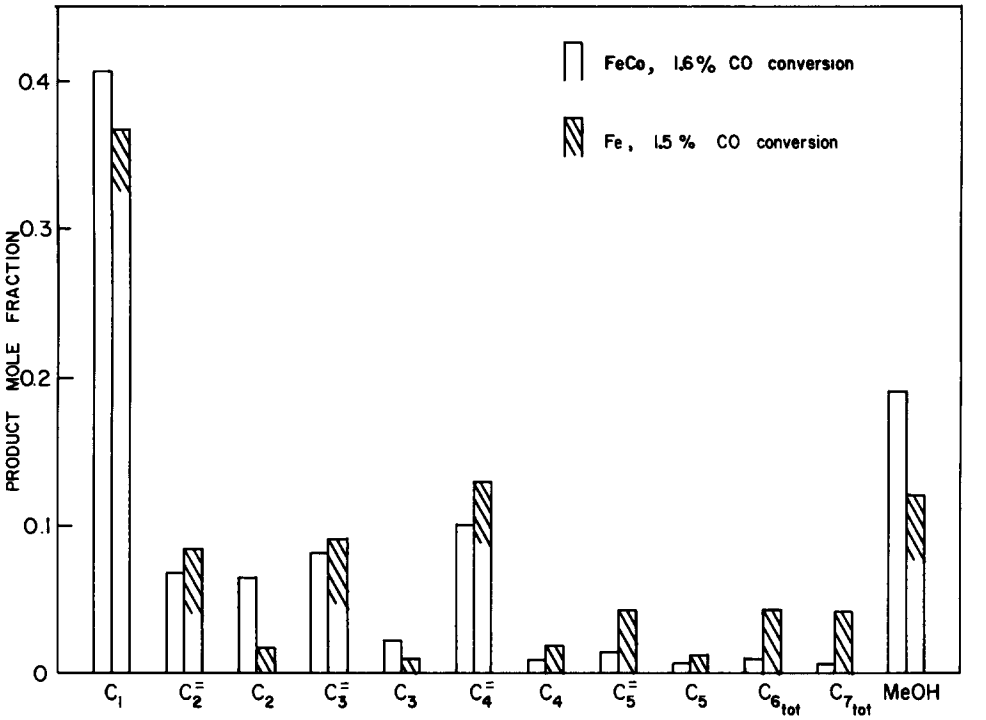

FIG. 15. Product mole fractions of the Fe and FeCo catalyst at 14 atm and 250°C with the 1/1 CO/H_2 feed.

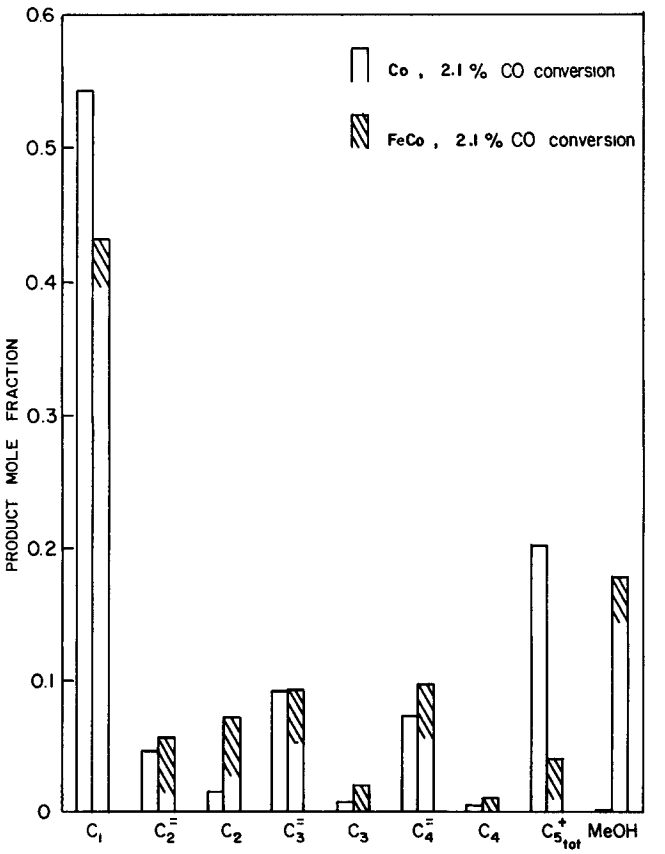

FIG. 16. Product mole fractions for the FeCo and Co catalyst at 7.8 atm and 250°C with the 1/1 CO/H_2 feed.

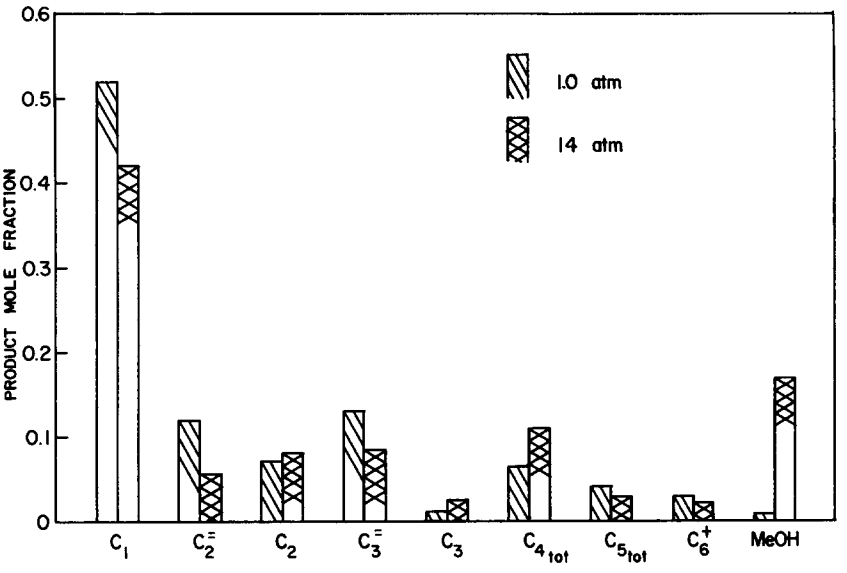

FIG. 17. Effect of increasing pressure on the product mole fraction of the FeCo catalyst at 2.7% CO conversion 1/1 CO/H_2 feed, 250°C.

perimental combinations investigated was with Fe, 14, 1/3. Co produced negligible amounts of methanol under any condition, however was efficient for longer chain hydrocarbons, as shown in Fig. 16.

The most significant effect of pressure in all of the experiments is the large increase in alcohol production, primarily at the expense of methane yield; typical results are shown in Fig. 17. (There is normally some decrease in C_4^- hydrocarbons as pressure increases together with a roughly equivalent increase in C_5^+.

Hydrocarbon Product Distribution

Hydrocarbon product distributions obeyed the chain propagation model:

$$\ln Y_j = n \ln \alpha + \ln \phi \qquad (2)$$

where Y_j is product yield, n is the number of carbon atoms in the product j, and α is the probability of chain growth.

Typical plots for the C_2^+ hydrocarbons are presented in Fig. 18 for the Co catalyst. The growth probability was independent of conversion level over the range studied, weakly dependent on feed composition and strongly dependent on total pressure. Figure 19 depicts the α dependence on total pressure for all three catalysts with both the 1/1 and 1/3 CO/H_2 feeds. Co/SiO_2, and to a

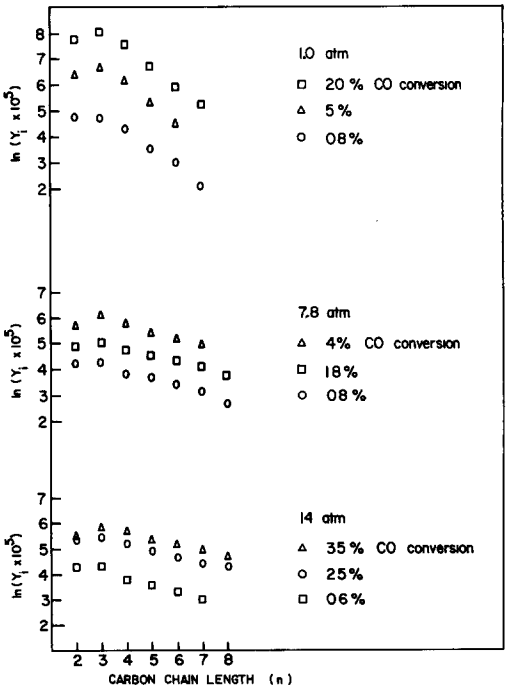

FIG. 18. Chain growth plots for the Co catalyst at 1 atm (top), 7.8 atm (middle), and 14 atm (bottom). 1/3 CO/H_2 feed at 250°C.

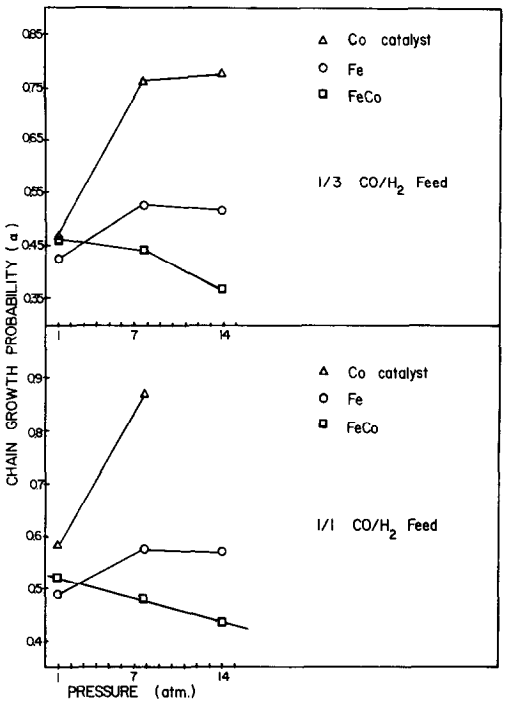

FIG. 19. Growth probabilities as a function of pressure for the 1/3 and 1/1 CO/H_2 feed mixtures.

lesser extent Fe/SiO_2, exhibit an increase in growth probability at higher pressures while α decreases for the alloy catalyst. At pressures greater than 1 atm the FeCo catalyst has a significantly lower growth probability than either pure component catalyst.

SUMMARY AND DISCUSSION

It is perhaps useful to give a summary here to draw into a broader perspective the results that have been presented. We do this in two parts (i) summary of the observed general behavior of the three catalysts in terms of pressure and feed composition and (ii) summary of the differences between the FeCo catalyst and the pure component materials.

The major observations with respect to the general behavior are as follows:

(1) Steady state CO activities decrease with increasing CO conversion and are higher for 1/3 CO/H_2 than for 1/1 CO/H_2.

(2) N_{CO} increases with pressure for Fe and FeCo, and decreases for Co. Overall, Co is the most active at 1 atm.

(3) Since there is no catalyst deactivation, the decrease in N_{CO} with conversion is due to product inhibition.

(4) N_{CH_4}/N_{CO} decreases both with increasing pressure and increasing CO conversion, and is lower for 1/1 than 1/3 feed ratios.

(5) Methanol becomes the second most dominant product at pressures above 1 atm for Fe and FeCo, and lower yields are obtained for 1/1 than for 1/3 feed ratios.

(6) There is a product inhibition effect on methanol production, although it is smaller than for overall N_{CO}.

(7) Shift activity decreases with increasing pressure, but under no condition is equilibrium-limited.

(8) Ethylene yield approaches a limiting value as CO conversion increases.

(9) Olefin/paraffin selectivities decrease with increasing conversion and pressure for all conditions studied.

(10) Hydrocarbon product distribution corresponds to the chain growth model for C_3^+ under all conditions; the chain growth probability is relatively insensitive to conversion but increases with increasing pressure. The 1/1 feed generally resulted in only marginal increases in the growth probability compared to 1/3 feed.

Observations with respect to the differences between the alloy catalyst and the pure component catalysts are as follows:

(1) FeCo has the lowest N_{CO} at 1 atm, however at higher pressures the overall activity increases to a level comparable with Co, though still less than Fe, for both feed mixtures.

(2) N_{CO} for the alloy catalyst appears to be proportional to the total pressure with 1/3 feed, but there is apparently a different kinetic dependence at lower CO/H_2 ratios.

(3) Enhanced methanol production with pressure increase is a property of both Fe and FeCo, with no methanol from Co. In ratio, Fe > FeCo for 1/3, and the reverse for 1/1 feed.

(4) Olefin/paraffin ratios are highest for FeCo at 1 atm, but they undergo the largest decrease of all the catalysts as pressure is increased.

(5) The FeCo catalyst has the smallest α value at higher pressures and generally produces the smallest product fraction (C_4^+) at the same conversion for equivalent conditions.

Much of the motivation for this study for the FeCo system was based on reports such as that of Nakamura *et al.* (*3*) claiming enhanced olefin selectivity for this material. The synergistic effect between Fe and Co was indeed observed by Amelse *et al.* (*5*) for FeCo, 1, 1/3. However, as shown by the present results the enhanced olefin selectivity is generally confined to these specific conditions, at least for the temperature employed here.

The fact that at higher pressures FeCo produces the largest amount of C_2 and C_3 paraffins and possesses the smallest growth probability, however, does provide some insight into the nature of the catalytic surface of the supported alloy. The CO activity of the alloy is at most 50% of the activity of Fe at any given set of reaction conditions; we take this as an indication that the surface of the alloy is depleted in iron concentration. At pressures greater than 1 atm the FeCo and Co catalysts have similar CO activities but their product distributions differ significantly. In fact, comparison of product distribution data (e.g., Figs. 5–7 and 14–16) indicates that at higher pressures the FeCo yields distributions similar to Fe but has the overall activity of the Co catalyst. There is thus a definite interaction between the components of the alloy since the activity/selectivity is not a simple combination of the pure component surfaces.

Amelse *et al.* (*5*) and Unmuth *et al.* (*7*) report characterization data that indicate the supported FeCo catalyst exists as a BCC alloy with a nonuniform composition with respect to particle size. This could explain the higher relative hydrogenation activity of the alloy catalyst since the surface associated with a Fe metallic phase can have higher hydrogenation activity than that associated with a carbidic phase, and FeCo does not form carbide phases under the conditions studied here.

However, the CO activity data and the hydrogenation data seem somewhat in conflict with each other, since the former yield the picture of a surface deficient in Fe with respect to the bulk composition and the latter could be interpreted as just the opposite. Different sites may be involved, though. The hydrogenation activity, coupled with the low growth probabilities of the alloy catalyst, may be indicative of a reaction sequence involving an ensemble (or ensembles) of surface atoms. If such ensembles, varying with particle size, include combinations of iron and cobalt atoms with different intrinsic surface rates there is no reason to expect any simple relationship between overall composition and catalyst activity and selectivity. Thus, the heterogeneity of catalyst composition may well play an important role in the observed contrasts in activity/selectivity.

The increase in methanol formation with increasing pressure for the alloy catalyst is clearly similar to that of Fe. This is possibly attributable to the presence of a larger amount of Fe^{2+} at higher pressures, stabilized by higher concentrations of H_2O and CO_2 even though the reaction atmosphere at the low conversions employed is still net reducing. This has been reported for other metals, in particular for Pd (*23*). This can be investigated via *in situ* Mössbauer reaction experiments that would certainly be of priority in further studies of the FeCo alloy system.

ACKNOWLEDGMENTS

This work was supported by the Department of Energy, Office of Basic Energy Sciences, Contract DE-AC02-78ER04993. The authors are indebted to R. L. Burwell, Jr., the reviewers of this paper, and W. K. Hall for helpful comments.

REFERENCES

1. Storch, H. H., Columbic, N., and Anderson, R. B., "The Fischer–Tropsch and Related Synthesis." Wiley, New York, 1951.
2. Vannice, M. A., and Garten, R. L., paper 17, 67th AIChE Meeting, Washington, D.C., December 1974.
3. Nakamura, M., Wood, B. J., Hou, P. Y., and Wise, H., "Proceedings, 7th International Congress on Catalysis, Tokyo," p. 432. Kodansha Ltd., Tokyo, 1981.
4. Unmuth, E. E., Ph.D. dissertation, Northwestern University, June 1979 (available from University Microfilms).
5. Amelse, J. A., Schwartz, L. H., and Butt, J. B., *J. Catal.* **72,** 95 (1981).
6. Amelse, J. A., Grynkewich, G., Butt, J. B., and Schwartz, L. H., *J. Phys. Chem.* **85,** 2484 (1981).
7. Unmuth, E. E., Schwartz, L. H., and Butt, J. B., *J. Catal.* **61,** 242 (1980).
8. Amelse, J. A., Schwartz, L. H., and Butt, J. B., *J. Phys. Chem.* **82,** 588 (1978).
9. McIlwrick, C., and Phillips, C., *J. Phys. E,* **6,** 1208 (1973).
10. Vannice, M. A., *Catal. Rev.-Sci. Eng.* **14,** 153 (1976).
11. Anderson, R. B., *in* "Catalysis", Vol. IV, Chap. 2, p. 29. (P. H. Emmett, Ed.), Reinhold, New York, 1956.
12. Atwood, H. E., and Bennett, C. O., *Ind. Eng. Chem. Process Des. Dev.* **18,** 163 (1979).
13. Dry, M. E., *Ind. Eng. Chem. Prod. Res. Dev.* **15,** 282 (1976).
14. Reymond, J. P., Meriaudeau, P., Pommier, B., and Bennett, C. O., *J. Catal.* **60,** 163 (1980).
15. Dwyer, D. J., and Somorjai, G. A., *J. Catal.* **52,** 291 (1978).
16. Neimantsverdriet, J. W., van der Kraan, A. M., van Dijik, W. L., and van der Baan, H. S., *J. Phys. Chem.* **84,** 3363 (1980).
17. Raupp, G. B., and Delgass, W. N., *J. Catal.* **58,** 361 (1979).
18. Ponec, V., and van Berneveld, W. A., *Ind. Eng. Chem. Prod. Res. Dev.* **18,** 268 (1979).
19. Kul'kova, N. V., and Temkin, M. I., *Zh. Fiz. Khim.* **23,** 695 (1949).
20. Dry, M. E., Shigles, T., and Boshoff, L. J., *J. Catal.* **25,** 99 (1972).
21. Stull, V. R., and Prophet, H., JANAF Thermochemical Tables, U.S. Government Printing Office, Washington, D.C., 1971 (2nd ed.).
22. Newsome, D. S., *Catal. Rev.-Sci. Eng.* **21,** 275 (1980).
23. Driessen, J. M., Poels, E. K., Hindermann, J. P., and Ponec, V., *J. Catal.* **82,** 26 (1983).